



HAL
open science

Design and control of a low-cost autonomous profiling float

Thomas Le Mézo, Gilles Le Maillot, Thierry Ropert, Luc Jaulin, Aurélien Ponte, Benoit Zerr

► **To cite this version:**

Thomas Le Mézo, Gilles Le Maillot, Thierry Ropert, Luc Jaulin, Aurélien Ponte, et al.. Design and control of a low-cost autonomous profiling float. 24^e Congrès Français de Mécanique, Aug 2019, Brest, France. hal-02276589

HAL Id: hal-02276589

<https://hal.science/hal-02276589>

Submitted on 2 Sep 2019

HAL is a multi-disciplinary open access archive for the deposit and dissemination of scientific research documents, whether they are published or not. The documents may come from teaching and research institutions in France or abroad, or from public or private research centers.

L'archive ouverte pluridisciplinaire **HAL**, est destinée au dépôt et à la diffusion de documents scientifiques de niveau recherche, publiés ou non, émanant des établissements d'enseignement et de recherche français ou étrangers, des laboratoires publics ou privés.

Design and control of a low-cost autonomous profiling float

Thomas Le Mézo^a, Gilles Le Maillot^a, Thierry Ropert^b, Luc Jaulin^a,
Aurélien Ponte^c, Benoît Zerr^a

a. ENSTA-Bretagne, Lab-STICC, 2 rue François Verny, 29806 Brest, France

b. ENSTA-Bretagne, Institut de Recherche Dupuy de Lôme (IRDL), 2 rue François Verny, 29806 Brest, France

c. Univ. Brest, CNRS, IRD, Ifremer, Laboratoire d'Océanographie Physique et Spatiale (LOPS), IUEM, Brest, France

Abstract

This paper presents the development made around the *SeaBot*, a new low-cost profiling float design for shallow water. We introduce a simplified dynamical model of the float and propose a state feedback depth controller coupled with an Extended Kalman Filter (EKF) to estimate model parameters. We show experimental results of the depth control that validate the model and the controller. We finally propose a loop design method to build low-cost floats by highlighting key design choices along with design rules.

Keywords : Float, state feedback, depth control, low-cost design, Extended Kalman Filter

Introduction

Profiling floats, which are a specific type of Autonomous Underwater Vehicle (AUV) that can only regulate their depth, are widely used in oceanography. They are equipped with instruments such as temperature, pressure, conductivity or biochemical sensors that measure the state of the water column. By carrying out profiles in the open ocean from the surface up to 3500 meters for the last generation, they help to a better understanding of the ocean and provide crucial data for oceanographic models through several years missions. The most well-known profiling floats are those of the Argo project [10, 12]: about 4000 floats that gather data continuously all over the world.

More recently, the oceanographic community has been focusing on swarm of profiling floats for shallow water [4, 5]. Indeed, in shallow water, the vertical and horizontal variation of biochemical parameters can be important. This is why increasing the density of data gathered is a key challenge to better understand submesoscales dynamics ($< 1 - 10\text{km}$).

Designing a low-cost profiling float that can conduct shallow water mission is then a key challenge. A low-cost float means a fast design and development phase, low or no calibration steps before using the float, a low cost per unit, while maintaining a high level of energetic and dynamical performances.

After introducing the dynamic model of a float, a focus will be given on the mechanical and electronic parts. A new command law based on a full state feedback coupled with an Extended Kalman Filter

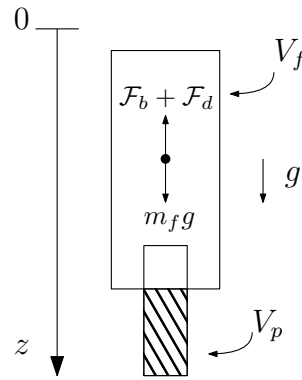


Figure 1: Float equipped with a piston system

(EKF) will then be introduced and validated with experimental trials. Finally, a loop iteration design will be presented which ensures that the key design choices are correctly chosen in order to build such floats.

Float dynamics

A profiling float controls its buoyancy to regulate its vertical position. There exists several mechanical systems to perform this task that either adjust the mass or the volume of the float. They are mainly based on hydraulic pump or piston system. Some float are also equipped with a passive system: they are design to stabilize themselves at a unique density.

We will consider here the case of a piston based system (see Figure 1). The principle is to adjust the volume of the float by pushing in or pulling out a piston that will modify the density and so the buoyancy. A float is primarily subject to gravity, buoyancy and drag forces. We make the assumption that the float has only vertical motion, with no rotation, that it is in thermal equilibrium with surrounding water, that the density of water is constant and that there is no vertical water velocity. A more complex model could be developed for more precise studies but a basic one seems to be sufficient to achieve an effective control (see Section 5). We have (see Table 1 for parameter descriptions):

$$(m_f + m_a)\ddot{z} = \mathcal{F}_b + \mathcal{F}_d - m_f g \quad (1)$$

where \mathcal{F}_b and \mathcal{F}_d are respectively the buoyancy force and the drag force. m_f is the mass of the float and m_a is the added mass which cannot be neglected in the case of water. The virtual mass $m_v = m_f + m_a$ is the sum of the two masses. We then have

$$m_v \ddot{z} = -\rho g V_t - \frac{1}{2} C_d S \rho |\dot{z}| \dot{z} - m_f g \quad (2)$$

where V_t is the total volume of the float composed of the sum of the piston volume V_p and the float volume V_f . Note that the volume of the float V_f is supposed to be equal at zero depth to m_f/ρ : the float has a neutral buoyancy. The piston volume V_p is then define as a positive or negative volume from neutral buoyancy at zero depth. (2) can then be simplified:

Parameter	Description	Unity	Typical <i>Seabot</i> value
\ddot{z}	float acceleration	m s^{-2}	
\dot{z}	float velocity	m s^{-1}	$[-0.3, 0.3]$
z	float depth	m	$[0, 50]$
m_v	virtual mass	kg	18
m_f	float mass	kg	9
m_a	added mass	kg	9
ρ	water density	kg m^{-3}	1025
g	acceleration due to gravity	m s^{-2}	9.81
V_t	total float volume	m^3	$V_f + V_p$
V_f	float volume	m^3	$\approx 8.8 \times 10^{-3}$
V_p	piston volume	m^3	$\Delta V_p = 1.7 \times 10^{-4}$
S	float's cross sectional area	m^2	4.5×10^{-2}
C_d	drag coefficient	–	1
\mathcal{K}_w	water compressibility	Pa^{-1}	4.27×10^{-10}
\mathcal{K}_f	float compressibility	Pa^{-1}	
χ	loss of volume per meter	$\text{m}^3 \text{m}^{-1}$	2.15×10^{-6}

Table 1: Float physical parameters

$$\begin{aligned}
m_v \ddot{z} &= -\rho g (V_f + V_p) - \frac{1}{2} C_d S \rho |\dot{z}| \dot{z} - \rho V_f g \\
\ddot{z} &= -\frac{\rho g}{m_v} V_p - \frac{C_d S \rho}{2 m_v} |\dot{z}| \dot{z}
\end{aligned} \tag{3}$$

A last phenomenon must be taken into account: the compressibility of the float. While increasing external pressure, the float's volume will decrease. This is also the case for water. The isothermal compressibility $\mathcal{K}_T = -\frac{1}{V} \left(\frac{\partial V}{\partial P} \right)_T$ measures the relative change of volume as a response to a pressure. We will assume that the water and float temperature are constant which means that \mathcal{K}_w , the water compressibility, and \mathcal{K}_f , the float compressibility are constants. We will also assume that the relation between pressure P and depth z is linear equal to $P(z) = \rho g z$.

We can then deduce the loss of buoyancy of the float which is explained by the relative variation of volume δV of the float compared to the equivalent one of water under the same pressure:

$$\mathcal{F}_{\mathcal{K}} = \rho g \delta V = \rho g (\mathcal{K}_f - \mathcal{K}_w) P(z) V_f = (\mathcal{K}_f - \mathcal{K}_w) m_f \rho g^2 z.$$

Note that we have neglected the loss associated to the piston volume and supposed the volume of the float constant. (3) can then be rewrite to take into account the compressibility:

$$\ddot{z} = -\frac{\rho g}{m_v} V_p - \frac{C_d S \rho}{2 m_v} |\dot{z}| \dot{z} + (\mathcal{K}_f - \mathcal{K}_w) \frac{m_f \rho g^2 z}{m_v}.$$

We set $\chi = m_f (\mathcal{K}_f - \mathcal{K}_w) g$, the loss of volume per meter depth, which is homogeneous to m^2 . We obtain

$$\ddot{z} = -\frac{\rho g}{m_v} (V_p - \chi z) - \frac{C_d S \rho}{2 m_v} |\dot{z}| \dot{z}.$$

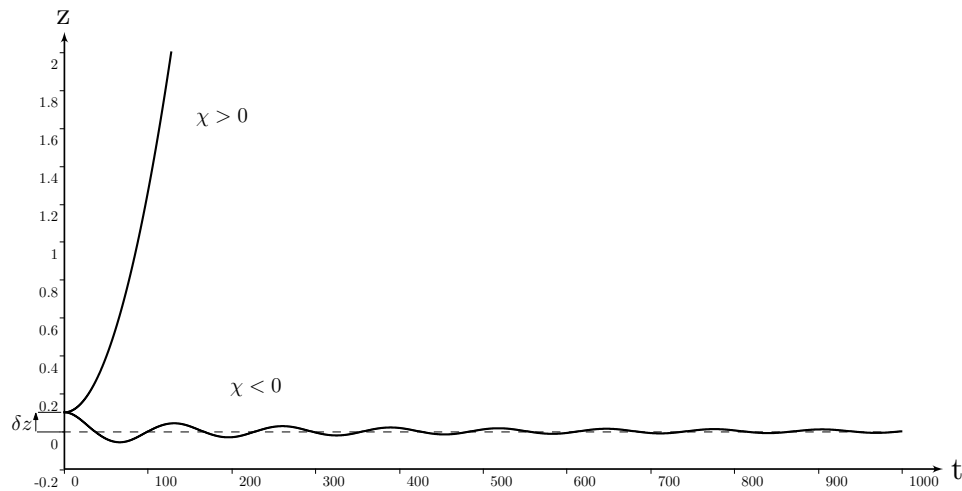


Figure 2: Evolution of float depth for a positive and a negative χ coefficient.

Set $A = \frac{\rho g}{m_v}$ and $B = \frac{C_d S \rho}{2m_v}$, we obtain:

$$\ddot{z} = -A(V_p - \chi z) - B|\dot{z}|\dot{z}. \quad (4)$$

The sign of the χ coefficient significantly affected the stability of the system. The float is stable for a negative χ and unstable for a positive value. Let the float be neutral buoyant for a depth z . If we moved it of δz , in the case of a negative χ , the variation of volume δV will be the same sign of δz which will produce a force in the opposite direction of the movement. The float will then go back to depth z . In the case of a positive χ the movement is on the contrary amplified by the variation of volume. Figure 2 shows the trajectory over time of two floats with a negative and positive χ . The float is stable for $z = 0$ and was moved of $\delta z = 0.1$ m. In the case of a negative χ the drag forces progressively reduce the oscillations while in the case of positive χ the system is clearly unstable and reach rapidly a constant positive velocity.

Robot design

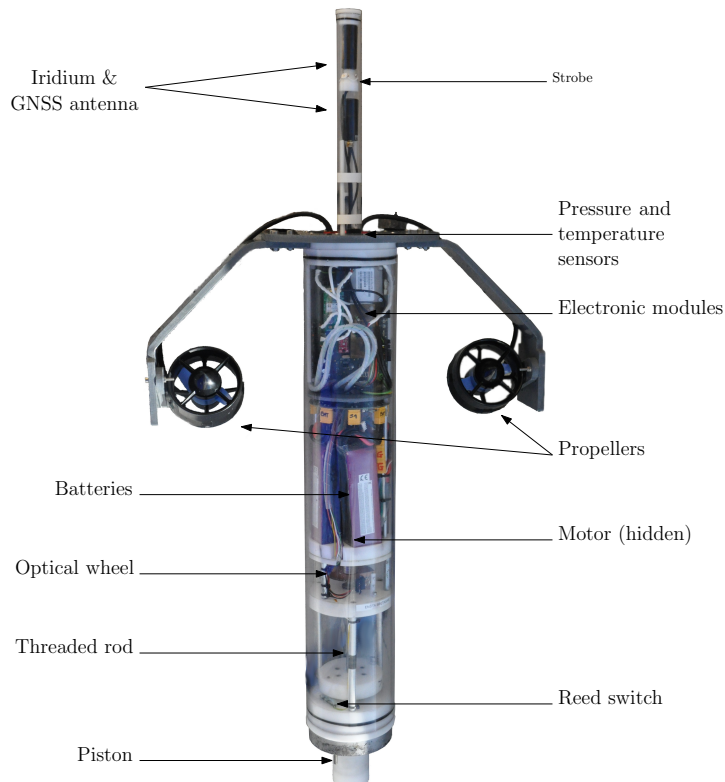
The *SeaBot* float is a 80cm low-cost system design for shallow water up to 50m (see Figure 3). The whole system was design in order to use as much as possible standard on the shelf mechanical and electronic components. We also tried to limit machining operations for manufacturing the float.

Mechanical system

In this subsection we will give an overview of the different design problems that have to be consider in order to build a low-cost float. The idea is to give simple first step design rules.

Float hull To avoid corrosion phenomenon and to facilitate the development of the float, we have chosen to use a full plastic hull and a transparent pipe. The caps and the piston are in polyoxymethylene (POM-C) and the pipe is in polycarbonate (PC).

To design the thickness of the pipe and the caps, we have to verify that [1, 2]:

Figure 3: The *Seabot* float

Material	Young modulus E	Elastic limit σ_e	Poisson's ratio ν	Density ρ
POM-C	2.8 GPa	67 MPa	0.35	1410 kg m ⁻³
PC	2.3 GPa	65 MPa	0.37	1200 kg m ⁻³
Stainless steel	190 GPa	170 MPa	0.3	8000 kg m ⁻³
Aluminum	69 GPa	30 MPa	0.35	2800 kg m ⁻³

Table 2: Approximate value of material mechanical properties

- $e_{\text{pipe}} > \frac{P \cdot d_{\text{pipe}}}{2\sigma_e}$ where e_{pipe} is the thickness of the pipe, P the external pressure, d_{pipe} the diameter of the pipe, σ_e the elastic limit and
- $e_{\text{caps}} > r_{\text{caps}} \sqrt{\frac{2}{3} \frac{P}{\sigma_e}}$ where r_{caps} is the radius of the caps.

In the case of the *SeaBot*, we obtain for a 50m depth limit and a 120mm pipe using Table 2, $e_{\text{pipe}} > 0.4$ mm and we choose a safety coefficient of more than 10 which gives a thickness of 5 mm. Concerning the caps, we obtain $e_{\text{caps}} > 8$ mm. Using stainless steel or aluminum would have allowed to reduce the thickness of the pipe to few millimeters but it raises issues with the propagation of wireless signal, the pipe ovalization at small thickness and the issue of galvanic corrosion. Moreover stainless steel is more dense than plastic materials, so the gain in thickness should be compared to the total mass.

Float compressibility Estimate the float compressibility is important to know if the system will be stable or unstable. At a first approximation, we can model the pipe by an infinite cylinder. We know from classical results [14, p.240] that the total radial travel for the external radius of a pressured thick-walled pipe is:

$$u = \frac{1 - \nu}{E} \frac{a^2 P_I - b^2 P_E}{b^2 - a^2} b + \frac{1 + \nu}{E} \frac{a^2 b^2 (P_I - P_E)}{(b^2 - a^2) b}$$

where u is the total radial travel, ν the poisson's ratio, E the young modulus, a the internal radius, b the external radius, P_E the external pressure and P_I the internal pressure.

If we neglect the effect of the two caps, the volume lost can be approximated by:

$$V_{\text{lost}} = \pi(b^2 - (b - u)^2)L$$

where L is the length of the pipe. We can then deduce an approximation of the float compressibility:

$$\mathcal{K}_f = -\frac{V_{\text{lost}}}{V_f P_E}$$

In the case of the *SeaBot* float, we obtain a mean compressibility for $P_E = 5$ bar, $P_I = 0.6$ bar and $L = 0.6$ m of $\mathcal{K}_f = 4.30 \times 10^{-9} \text{ Pa}^{-1}$. We can then deduce the loss of volume per meter $\chi = 7.22 \times 10^{-7} \text{ m}^3 \text{ m}^{-1}$. The float is found to be unstable.

The χ_{theory} is similar to the $\chi_{\text{measured}} \simeq 2.14 \times 10^{-6} \text{ m}^3 \text{ m}^{-1}$. A more detailed study using numerical simulation should be undertaken to obtain a better estimation of the χ_{theory} . By comparison, a 2 mm thick aluminum pipe would have been less compressible than water.

Auto-ballasting system The auto-ballasting system (ABS) is based on a 5cm diameter piston that moves along a M12 steel threaded rod which is rotated with a brushed motor. The position of the piston is given by an optical codewheel (48 counts per revolution) and two reed switch that provide a mechanical zero position reference.

The required torque that the motor has to deliver can be calculated classically [1, 2] by the following equation:

$$\mathcal{T} = F_P r_{\text{mean}} \tan(i + \varphi) \quad (5)$$

where \mathcal{T} is the torque (in $N \cdot m$), F_P is force normal force applied on the piston (in N), r_{mean} the mean radius of the threaded rod (in m), i the thread angle and φ the angle of friction that depends on the materials.

In the *SeaBot* case, we have $F_P = \rho g z_{\text{max}} S$, $r_{\text{mean}} = 6\text{mm}$, the screw thread is 1.75mm which gives $i = 8^\circ$ and if we assume a friction coefficient of 0.4 between steel and POM-C, $\varphi = 22^\circ$. We obtain $\mathcal{T}_{\text{max}} = 3.4 \text{ Nm}$.

The *SeaBot* motor is a $\mathcal{P}_m = 19.8 \text{ W}$ MFA Como 970D1561 of 0.015 Nm at maximum efficiency and 0.1 Nm at the maximum torque, with a 156:1 reduction gearbox, which gives a maximum output torque between 2.34 Nm and 15.6 Nm $> \mathcal{T}_{\text{max}}$. The output rotation speed is 93RPM so we can compute the theoretical maximum volume variation of the piston per time: $\dot{V}_p = 5.32 \times 10^{-6} \text{ m}^3 \text{ s}^{-1}$.

A compromise has to be found between the diameter of the piston, the maximum torque of the motor and the maximum volume rate of the piston.

Propellers The *SeaBot* float is also equipped with two low-cost propellers that can be used at surface to correct a position drift due to currents.

Depressurization The internal part of the float is maintain at a pressure of 600mBar. This vacuum maintains the O-rings and the two caps. This also provides an easy way to detect leak issue.

Electronic system

Electronic design The main electronic is based on a Raspberry Pi 3 B+ board and microcontrollers dedicated to real time control and hardware interfaces.

Sensors The float is equipped with a 18 cm accuracy pressure sensor (89BSD TE), an external temperature sensor, a MEMS IMU, a GNSS receiver and Iridium transceiver, an optical codewheel for the piston and an internal temperature, pressure and humidity sensor to detect water leak issues. Monitoring the humidity level appears to be more efficient to detect small leaks than monitoring the internal pressure which requires important water ingress to change.

Energy The float has four 5Ah 3S LiPo batteries that provide a total of 20 Ah. This gives around 226Wh and about a one day autonomy. The electronic system without the motor and propellers consumes around 2.5W. The electronic energy consumption can be greatly optimized in a second step design.

Depth controller

Implementing an efficient control law that minimize the energy consumption while maintaining a low error relative to the depth set point is challenging in the context of low-cost actuators and sensors. Several approach has been used: a survey of profiling float controllers can be found in [13]. Classical PID based controllers are not suitable in the context of low-cost floats as underlined in [11] because of the time required to tune experimentally their coefficients. State of the art float controller now use state feedback controllers [4] or adaptive control [3]. The main difficulty of those controllers is the ability to know an accurate dynamical model. Indeed, several parameters such as buoyancy depends of surrounding water properties such as density: an online estimation must then be implemented. To solve the problem, several techniques have been used including fuzzy inferences [4] or full state observers [11].

In the following section we will propose a new method base on a state feedback controller and an online estimator based on an Extended Kalman Filter (EKF).

The float system can be model through the following equation: $\dot{\mathbf{x}} = \mathbf{f}(\mathbf{x}, \mathbf{u})$ where \mathbf{x} is the state vector of the system, \mathbf{f} the evolution function of the system and \mathbf{u} the command. From equation (4), we obtain:

$$\dot{\mathbf{x}} = \begin{pmatrix} \dot{z} \\ \dot{z} \\ \dot{V}_p \end{pmatrix} = \begin{pmatrix} -A(V_p - \chi z) - B|\dot{z}| \dot{z} \\ \dot{z} \\ u \end{pmatrix} \quad (6)$$

where u is the piston volume rate.

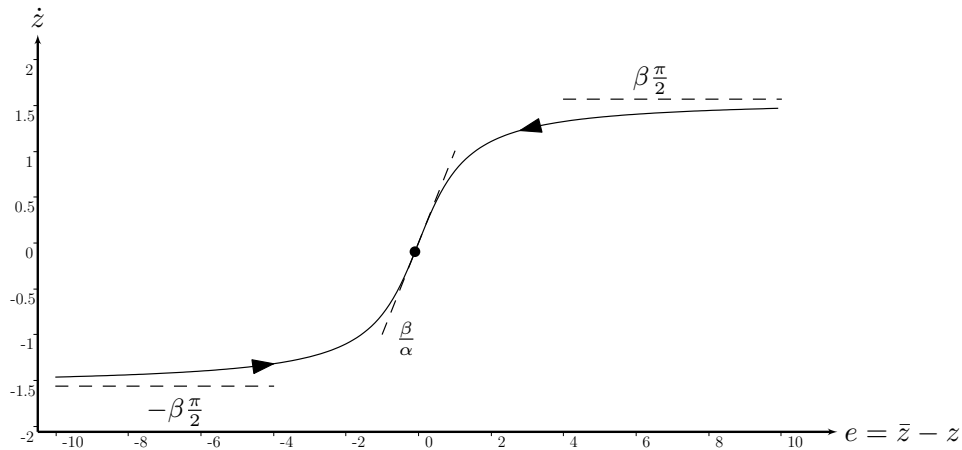


Figure 4: Map of the set-point velocity as a function of the depth error e

Command law

In a context of low energy consumption, we want to avoid as much as possible any overshoot of the command which would cause unnecessary movements of the piston. In term of energy, the mechanical work of the piston depends of the velocity and of the loss of volume per meter χ . If $\chi = 0$, the float can move from an equilibrium depth position to an other with an ε move of the piston: the work is then directly link to the velocity of the movement and not to the travelled depth.

To be able to limit the velocity while reaching the desired depth, we chose to control the float with a vector field that link the velocity and the depth error to the set-point (see Figure 4):

$$\dot{z} = \beta \arctan\left(\frac{\bar{z} - z}{\alpha}\right)$$

where \bar{z} is the set-point depth and (α, β) is a pair of two constant parameters. Other functions such as sigmoids could have been chosen as long as they are smooth which is required to apply state feedback techniques. The coefficients α and β will be chosen depending on the performances required by the user application in particular the max velocity $\dot{z}_{\max} = \beta \frac{\pi}{2}$ and the deceleration phase near the depth set point though $\frac{\beta}{\alpha}$. The adjustment of these parameters will be discuss in subsection 4.3.

To apply state feedback linearization technique [6], we chose for the system output $y = \dot{z} - \beta \arctan\left(\frac{\bar{z} - z}{\alpha}\right)$. Our system has a relative degree of 2 which requires to derive two times the output.

$$\dot{y} = \ddot{z} - \frac{\beta}{\alpha} \frac{-\dot{z}}{1+e^2} = \ddot{z} - \gamma \frac{-\dot{z}}{D}$$

where $e = \frac{1}{\alpha}(\bar{z} - z)$, $D = 1 + e^2$, $\gamma = \frac{\beta}{\alpha}$,

$$\ddot{y} = \dddot{z} + \gamma \frac{\ddot{z}D - \dot{z}\dot{D}}{D^2} = \dddot{z} + \gamma \frac{\ddot{z}D + 2\alpha^{-2}e\dot{z}^2}{D^2}$$

as $\dot{D} = -2\alpha^{-2}e\dot{z}$ and with $\ddot{z} = -A(u - \chi\dot{z}) - 2B|\dot{z}|\dot{z}$,

$$\ddot{y} = -Au + A\chi\dot{z} - 2B|\dot{z}|\ddot{z} + \gamma \frac{\ddot{z}D + 2\alpha^{-2}e\dot{z}^2}{D^2}.$$

We then chose u such that y is solution of $\lambda_3\ddot{y} + \lambda_2\dot{y} + \lambda_1y = 0$ where $\lambda_1, \lambda_2, \lambda_3$ are constant coefficients. In order to avoid any overshoot we want a single negative pole s such that the characteristic equation of the previous equality is $(1-s)^2$, which give the coefficient values: $\lambda_3 = 1$, $\lambda_2 = -2s$ and $\lambda_1 = s^2$. The command u can be then expressed as:

$$u = \frac{1}{A}(-2s\dot{y} + s^2y + \gamma \frac{\ddot{z}D + 2\alpha^{-2}e\dot{z}^2}{D^2} - 2B|\dot{z}|\ddot{z}) + \chi\dot{z}.$$

This allows y to converge towards 0 at a speed of $\sim e^{st}$. The pole s should be chosen in function of the dynamic of the system. The previous model is only valid when the float is completely immersed. This is not the case at surface when antennas are emerged. This is why a simple finite-state machine switch between a simple sink procedure that slowly retract the piston until a certain depth z_f is reached where the state feedback controller is then activated.

Estimation of unknown parameters

The main issue with the control law described above is that the exact volume V_p of the piston and the χ parameter are unknown. Concerning the volume, we measure with a high precision the volume of the piston V_m from a mechanical zero reference but we do not know the offset V_o such that the float is at equilibrium at zero depth ($V_p = V_m + V_o$). The parameter χ is even more complex to estimate as it also depends of surrounding water properties.

This is why an EKF will be used to estimate V_o and χ . Note that some of the modeling errors would be also compensated by the estimation of both variables. By using equation (6), we can obtain a specific system for the estimation of V_o and χ . Note that V_p is here consider as the input u , we measure z and we suppose that V_o and χ are constant over time. With the state vector $\mathbf{x} = (\dot{z}, z, V_o, \chi)^T$, we have for the continuous system:

$$\begin{cases} \dot{\mathbf{x}} = \mathbf{f}_c(\mathbf{x}, u) & = \begin{pmatrix} -A(u - \chi z) - B|\dot{z}|\dot{z} \\ \dot{z} \\ 0 \\ 0 \end{pmatrix} \\ \mathbf{y} = \mathbf{g}(\mathbf{x}) & = (z) \end{cases} \quad (7)$$

We recall the Kalman prediction and corrector equations in the case of a discrete time system, with an euler integration scheme at step k and a dt duration between steps. Notations are taken from [6]:

- Prediction $\begin{cases} \hat{\mathbf{x}}_{k+1|k} = \mathbf{f}(\hat{\mathbf{x}}_{k|k}, \mathbf{u}_k) = \hat{\mathbf{x}}_{k|k} + dt \cdot \mathbf{f}_c(\mathbf{x}_k, \mathbf{u}_k) & \text{(predicted estimation)} \\ \Gamma_{k+1|k} = \mathbf{A}_k \cdot \Gamma_{k|k} \cdot \mathbf{A}_k^T + \Gamma_{\alpha_k} & \text{(predicted covariance)} \end{cases}$

Parameter	Lower bound	Upper bound
V_p	$-2.148 \times 10^{-5} \text{ m}^3$	$1.503 \times 10^{-4} \text{ m}^3$
\dot{V}_p	$-1.431 \times 10^{-6} \text{ m}^3 \text{ s}^{-1}$	$1.431 \times 10^{-6} \text{ m}^3 \text{ s}^{-1}$

Table 3: *Seabot* piston parameters (experimental results, \dot{V}_p is limited by software compare to the maximum possible values)

$$\bullet \text{ Update } \begin{cases} \hat{\mathbf{x}}_{k|k} = \hat{\mathbf{x}}_{k|k-1} + \mathbf{K}_k \tilde{\mathbf{z}}_k & \text{(corrected estimation)} \\ \Gamma_{k|k} = (\mathbf{I} - \mathbf{K}_k \mathbf{C}_k) \Gamma_{k|k-1} & \text{(corrected covariance)} \\ \tilde{\mathbf{z}}_k = \mathbf{y}_k - \mathbf{C}_k \hat{\mathbf{x}}_{k|k-1} & \text{(innovation)} \\ \mathbf{S}_k = \mathbf{C}_k \Gamma_{k|k-1} \mathbf{C}_k^T + \Gamma_{\beta_k} & \text{(covariance of the innovation)} \\ \mathbf{K}_k = \Gamma_{k|k-1} \mathbf{C}_k^T \mathbf{S}_k^{-1} & \text{(Kalman gain)} \end{cases}$$

where

$$\bullet \mathbf{A}_k = \frac{\partial \mathbf{f}(\hat{\mathbf{x}}_{k|k}, \mathbf{u}_k)}{\partial \mathbf{x}} = \begin{pmatrix} -2B|\hat{z}| & A\hat{\chi} & -A & A\hat{z} \\ 1 & 0 & 0 & 0 \\ 0 & 0 & 0 & 0 \\ 0 & 0 & 0 & 0 \end{pmatrix} \cdot dt + \mathbf{I}_{4 \times 4} \text{ is the evolution matrix,}$$

$$\bullet \mathbf{C}_k = \frac{dg(\hat{\mathbf{x}}_{k|k-1})}{dx} = \begin{pmatrix} 0 & 1 & 0 & 0 \end{pmatrix} \text{ is the observation matrix,}$$

- and Γ_{α} , Γ_{β} are respectively the process and the observation noise covariance matrices. In our case we set them diagonal and constant. Their coefficients depends of the sensors accuracy and of the dynamic of the float.

Validation of the command law and application to the *SeaBot* float

The float has mechanical constraints which bounds the volume $V_p \in [V_p^-, V_p^+] = [V_p]$ and the volume rate of the piston $\dot{V}_p \in [\dot{V}_p^-, \dot{V}_p^+] = [\dot{V}_p]$. In this subsection we will discuss how these constraints narrow the α, β, s and \bar{z} possible values.

The parameters for the *SeaBot* piston are summarized in Table 3. The asymmetry between V_p^+ and V_p^- is due to the need to have a sufficient reserve buoyancy to emerge antennas.

Maximum depth The maximum depth is not only limited by the hull durability against pressure but also by the loss of volume due to compressibility. At equilibrium in the case of the maximum depth, we have from (4): $V_p - \chi z_{\max} = 0$ which implies that $z_{\max} = \max \left(\frac{V_p}{\chi} \right)_{V_p \in [V_p]}$. For a stable float ($\chi < 0$), the float will not be able to go deeper. Whereas for an unstable float, it will not be able to go back to a lower depth if it goes deeper to this limit.

The maximum theoretical depth due to the piston volume for the *SeaBot* is $z_{\max} = 70\text{m}$. Under this limit, there won't be enough reserve buoyancy to come back to surface. The limit for the *SeaBot* was set to $z_{\max} = 50\text{m}$ which also take into account the mechanical strength of the pipe.

Maximum velocity The maximum reachable velocity \dot{z}_{\max} depends of the depth due to compressibility. If we suppose that the float has stabilized its velocity to \dot{z}_{\max} , we then have from 4: $-A(V_p - \chi z) - B|\dot{z}_{\max}| \dot{z}_{\max} = 0$ which implies that

$$\dot{z}_{\max|z} = \left(\sqrt{\left| \frac{A}{B} (V_p - \chi z) \right|} \right)_{V_p \in \{V_p^-, V_p^+\}} \quad (8)$$

In the case of the *SeaBot*, we obtain

$$\begin{cases} \dot{z}_{\max|z=0} \in \{-0.255, 0.097\} \text{ m s}^{-1} \\ \dot{z}_{\max|z=50} \in \{-0.136, 0.236\} \text{ m s}^{-1} \end{cases}$$

This is consistent with the fact that at surface there is more positive reserve buoyancy than negative one that explain the difference of velocity. The phenomenon is reversed at 50m due to the loss of volume. Note that these maximum velocities are only based on the hypothesis of stabilized velocity: higher values can be reached for a depth z depending of the previous trajectory and drag forces. Moreover, the drag coefficient was not estimate accurately so this values only give an order of magnitude.

Note also that the maximum velocity is limited by $[\dot{V}_p]$ as the piston has to move faster than the loss of volume due to compressibility. Otherwise, in the case of an unstable float, it will not succeed in decelerating, and in the stable case, the velocity will be limited. $\dot{z}_{\max} = \frac{\dot{V}_p}{\chi} |_{\dot{V}_p \in \{\dot{V}_p^-, \dot{V}_p^+\}} \in \{-0.66, 0.66\} \text{ m s}^{-1}$.

Vector field following An important issue is to verify that the maximum piston volume rate \dot{V}_p is sufficient to follow the imposed trajectory. When the float is stabilized on the trajectory [8], we know that $\dot{z} = \beta \arctan\left(\frac{\bar{z}-z}{\alpha}\right)$, we also know that $\dot{y} = 0$ so $\ddot{z} = \gamma \frac{-\dot{z}}{D}$ which implies that $V_p = \frac{1}{A} \left(\frac{\gamma \dot{z}}{D} + B|\dot{z}| \dot{z} \right) + \chi z$. We can then compute u as a function of z as we know \dot{z} and V_p in function of z . In order to obtain a guaranteed evaluation of $u(z)$ and avoid numerical errors, we will use interval techniques [7] to bracket the function such that $u \in [u^-, u^+]$.

If we take $s = -1, \beta = 0.05 \frac{2}{\pi}, \alpha = 1$ and $\bar{z} = 0$, we obtain Figure 5. We can see that the command is always inside the maximum and minimum piston volume rate. We can clearly see that when the system is far from the target, it needs to compensate χ . The local increase of u near the setpoint is due to the deceleration. The maximum volume velocities computed are $\{-1.383 \times 10^{-7}, 1.383 \times 10^{-7}\} \text{ m}^3 \text{ s}^{-1}$.

We can also study the impact of the command near the desired velocity set-point. If we assume that $\dot{z} = \beta \arctan\left(\frac{\bar{z}-z}{\alpha}\right) + w$ where $w \in [-5 \times 10^{-3}, 5 \times 10^{-3}] \text{ m s}^{-1}$ and for $s = 0.1$, we obtain the dotted curves of Figure 5 and the new maximum volume velocities: $\{-5.62 \times 10^{-7}, 5.62 \times 10^{-7}\} \text{ m s}^{-1}$.

The study of the transition phase where the system reach the vector field is also an important key-point that is not studied here. More generally, the computation of the largest positive invariant set [9] of the system in a context of a saturated command would be interesting. This means to find the set of all states from which the system will converge to the depth set-point. A sufficient reserve of \dot{V}_p must be preserved to efficiently backtrack the correct velocity.

Minimum piston volume increment Defining the minimum codewheel step increment is a difficult task. A way to estimate a minimum value is to evaluate from equation 8 a step of piston volume from an error velocity.

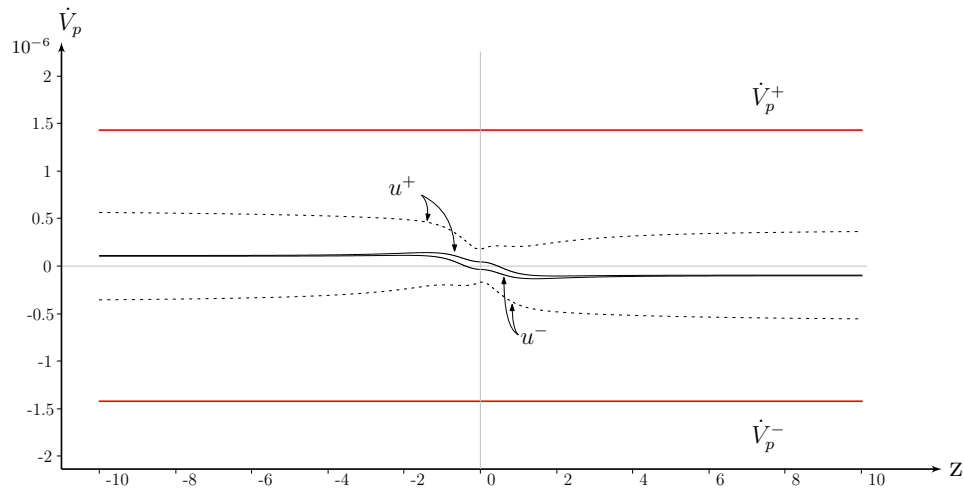


Figure 5: Outer approximation of the command in function of depth for two configurations. The maximum bound of \dot{V}_p are in red.

In the case of the *SeaBot*, if we allow a $\delta\dot{z} = 0.01 \text{ m s}^{-1}$ velocity error at zero depth, it is equivalent to an error of volume of $\delta V_p = 2.306 \times 10^{-7} \text{ m}^3$. We have chosen a 48 counts per revolution codewheel which gives a $\delta V_p = 7.16 \times 10^{-8} \text{ m}^3$.

Energy consumption For a given maximum velocity \dot{z}_m and a depth change Δz with a zero velocity at the beginning and end, we can deduce the variation of piston volume. By taking into account the piston volume rate, we can obtain the amount of motor run time if we suppose at a first approximation a one step variation. We can then deduce an under approximation of the power required for the trajectory:

$$\mathcal{E} = \frac{\Delta V_p}{\dot{V}_{p,\max}} \mathcal{P}_m = \frac{2 \left(\frac{B}{A} \dot{z}_m^2 \right) + |\chi \Delta z|}{\dot{V}_{p,\max}} \mathcal{P}_m$$

We assume here, to simplify, that the piston volume change for the velocity and for the loss of volume are independent. We also assume that the piston has to first move to reach \dot{z}_m and then to move to decelerate to zero velocity.

In the case of the *SeaBot*, for a $\Delta z = 50 \text{ m}$ and $\dot{z}_m = 0.05 \text{ m s}^{-1}$, we obtain a run time of 83s and $\mathcal{E} = 0.457 \text{ Wh}$.

Experimental results

The float system was tested in a 20m deep sea water basin at IFREMER Brest (see Figure 6). The state feedback controller and the EKF were running at 5 Hz with a transition depth $z_f = 0.3 \text{ m}$. The mission was to reach five different depth levels $\{1, 5, 10, 15, 18\} \text{ m}$ with a maximum speed of $|\dot{z}_{\max}| = 0.04 \text{ m s}^{-1}$, $\alpha = 1$ and $s = -1$. Figure 7 shows the trajectory over time and Figure 8 shows the piston volume measured V_m . There is no overshoot of the command and we clearly see the compensation of the loss of volume on the volume V_m : the deeper the float is the more volume the piston has to be pushed out.

Evolution of χ Measuring the volume of the piston once the float is stabilized at every depth level give an idea of the value of χ . From experimental data, the loss of volume appears not to be linear with

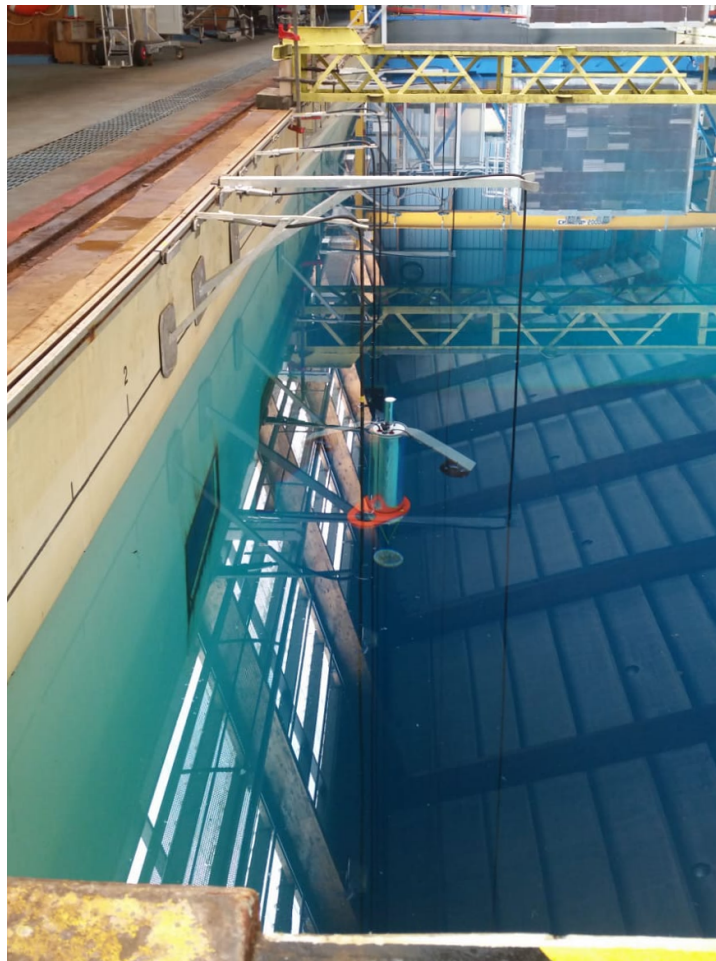
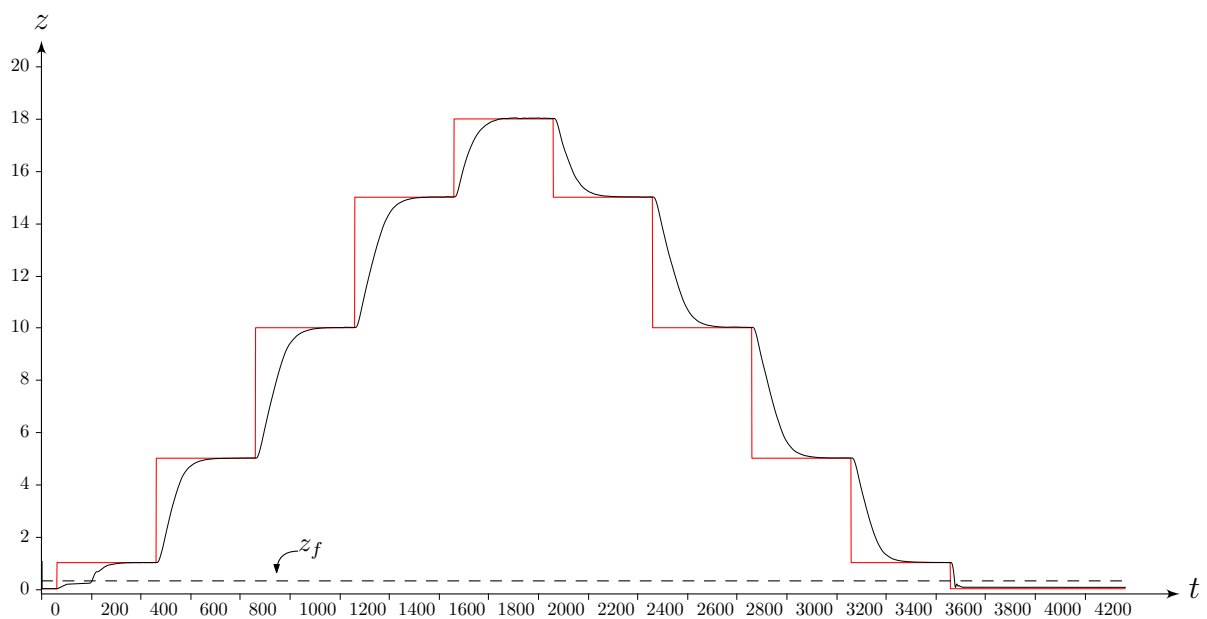
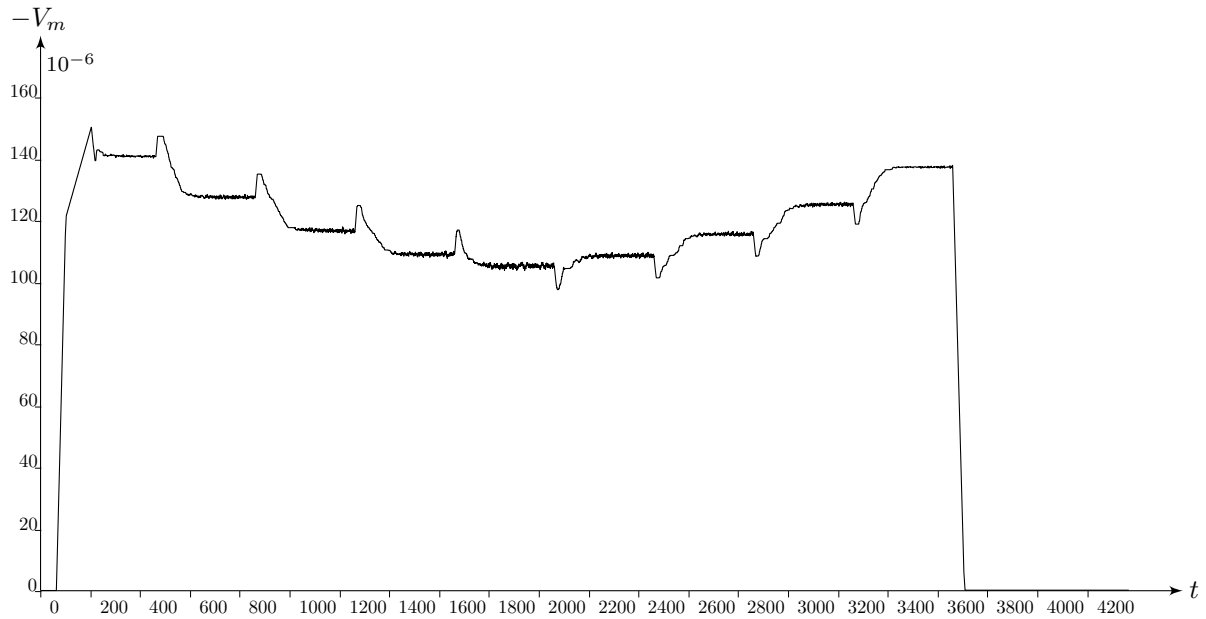
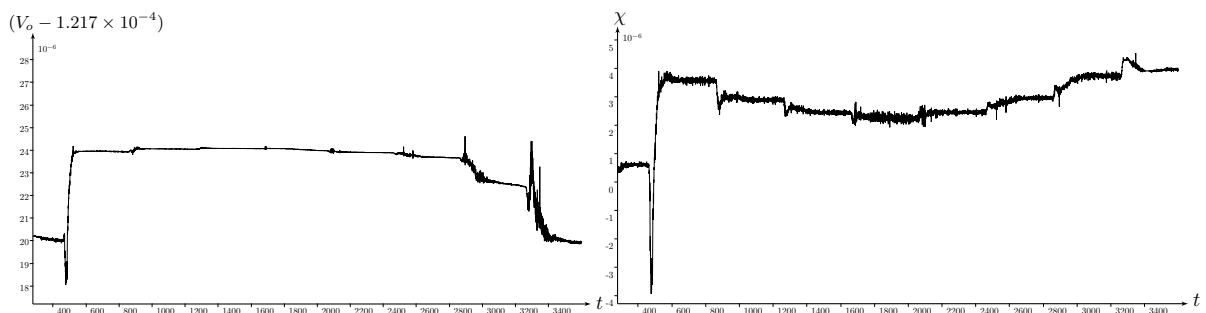


Figure 6: Trials at IFREMER basin.

Figure 7: Depth z (in meter) of the float in function of time t (in seconds). The setpoint trajectory is in red and the float trajectory is in black.

Figure 8: Piston volume measured V_m in function of time t (in seconds)Figure 9: Estimation of V_0 and χ by the EKF over time

depth z but quadratic with respect to z . However the EKF handles this model error and adjust the value of χ and V_0 (see Figure 9).

Energy consumption To reduce the energy consumption during ascending and descending phases, we compute an interval of command $[u]$ for an interval of maximum velocity $[\dot{z}_{\max}]$ and we chose the command that minimize $|u|$. A no piston movement strategy could also be adopted when the set-point is reached in the case of a stable float but this is not the case for our system.

Depth error The depth error while the depth level is reached is of few centimeters (in most cases under 2 cm). Some depth bias of up to 4 cm can be observed which could come from mechanical hysteresis or error in the model. Adding an integral effect to the control law is a solution to compensate these small bias.

Design loop

Similarly to the ship design loop technique from the Naval Architecture community, we propose here a low-cost float design loop. The idea is to compute from the problem inputs, the minimum electronic

and mechanical characteristics of the float.

- Problem inputs:
 - mass of the payload: m_p ,
 - maximum float velocity required \dot{z}_{\max} , trajectory to follow and error allowed,
 - volume of the antennas V_a ,
 - max depth: z_m ,
 - mission duration T and number of typical depth variation Δz .
- Design loop
 1. Compute the diameter b and length L of the float (function of m_p). Choose a material for the hull and compute its minimum thickness (function of z_m).
 2. Estimate the damping coefficient D (function of b) and the loss of volume per meter χ .
 3. Compute the volume of the piston $[V_p]$ required to (i) emerge antennas (V_a), (ii) compensate the loss of volume (χ), (iii) and reach the maximum velocity (function of D).
 4. Compute the velocity of the piston $[\dot{V}_p]$ required to follow the trajectory and compensate χ . Set the minimum motor specifications.
 5. Compute the step increment of piston volume (δV) and choose a depth sensor according to specifications.
 6. Estimate the power consumption and choose the battery capacity.
 7. Go to step 1 if energy autonomy does not comply with the maximum payload weight.

Conclusion

In this paper, we presented a new low-cost profiling float called *SeaBot*. It implements a new method based on a full state feedback controller and EKF estimator that was tested experimentally. We also presented tools to validate the system characteristics and proposed a design loop to develop low-cost float.

Acknowledgment

This work has been supported by the *French Government Defense procurement and technology agency* (DGA).

References

- [1] P. Agati, F. Lerouge, and M. Rossetto. *Résistance des matériaux - 2^{ème} édition - Cours, exercices et applications industrielles*. 2e édition. Paris: Dunod, 2008. 512 pp. ISBN: 978-2-10-051634-6.
- [2] M. Aublin et al. *Systèmes mécaniques - Théorie et dimensionnement*. Paris: Dunod, 2005. 688 pp. ISBN: 978-2-10-049104-9.
- [3] E. J. Berkenpas et al. "A Buoyancy-Controlled Lagrangian Camera Platform for In Situ Imaging of Marine Organisms in Midwater Scattering Layers". In: *IEEE Journal of Oceanic Engineering* 43.3 (July 2018), pp. 595–607. ISSN: 0364-9059.

- [4] W. M. Bessa et al. “Design and Adaptive Depth Control of a Micro Diving Agent”. In: *IEEE Robotics and Automation Letters* 2.4 (Oct. 2017), pp. 1871–1877. ISSN: 2377-3766.
- [5] J. S. Jaffe et al. “A swarm of autonomous miniature underwater robot drifters for exploring sub-mesoscale ocean dynamics”. In: *Nature Communications* 8 (Jan. 24, 2017), p. 14189. ISSN: 2041-1723.
- [6] L. Jaulin. *Mobile Robotics*. Ed. by ISTE. Mobile Robotics. Nov. 2015.
- [7] L. Jaulin et al. *Applied Interval Analysis: With Examples in Parameter and State Estimation, Robust Control and Robotics*. London: Springer-Verlag, 2001. ISBN: 978-1-85233-219-8.
- [8] M. Le Gallic et al. “Tight slalom control for sailboat robots”. In: International Robotic Sailing Conference (IRSC). Aug. 31, 2018.
- [9] T. Le Mézo, L. Jaulin, and B. Zerr. “An Interval Approach to Compute Invariant Sets”. In: *IEEE Transactions on Automatic Control* 62.8 (Aug. 2017), pp. 4236–4242. ISSN: 0018-9286.
- [10] S. Le Reste et al. ““Deep-Arvor”: A new profiling float to extend the Argo observations down to 4000m depth.” In: *Journal Of Atmospheric And Oceanic Technology* 33.5 (May 1, 2016), pp. 1039–1055. ISSN: 0739-0572.
- [11] B. McGilvray and C. Roman. “Control system performance and efficiency for a mid-depth Lagrangian profiling float”. In: *OCEANS’10 IEEE SYDNEY*. OCEANS’10 IEEE SYDNEY. May 2010, pp. 1–10.
- [12] S. C. Riser et al. “Fifteen years of ocean observations with the global Argo array”. In: *Nature Climate Change* 6.2 (Feb. 2016), pp. 145–153. ISSN: 1758-6798.
- [13] Y. Shi et al. “Advanced Control in Marine Mechatronic Systems: A Survey”. In: *IEEE/ASME Transactions on Mechatronics* 22.3 (June 2017), pp. 1121–1131. ISSN: 1083-4435.
- [14] S. Timoshenko. “Strength of Materials, Part II”. In: *Advanced Theory and Problems* 245 (1941).